# Assessment of GPS global ionosphere maps (GIM) by comparison between CODE GIM and TOPEX/Jason TEC data: Ionospheric perspective

G. Jee,[1] H.-B. Lee,[1,2] Y. H. Kim,[3] J.-K. Chung,[4] and J. Cho[4]

Received 7 March 2010; revised 25 May 2010; accepted 15 June 2010; published 23 October 2010.

[1] We performed a comprehensive comparison between GPS global ionosphere map (GIM) and TOPEX/Jason (T-J) total electron content (TEC) data for the periods of 1998–2009 in order to assess the performance of GIM over the global ocean where the GPS ground stations are very sparse. Using the GIM model constructed by the Center for Orbit Determination in Europe at the University of Bern, the GIM TEC values were obtained along the T-J satellite orbit at specific locations and times of measurements and then binned into various geophysical conditions for direct comparison with the T-J TEC. On the whole, the GIM model was able to reproduce the spatial and temporal variations of the global ionosphere as well as the seasonal variations. However, the GIM model was not accurate enough to represent the well-known ionospheric structures such as the equatorial anomaly, the Weddell Sea Anomaly, and the longitudinal wave structure. Furthermore, a fundamental limitation of the model seems to be evident in the unexpected negative differences (i.e., GPS < T-J) in the northern high-latitude and the southern middle- and high-latitude regions in comparison with the T-J TECS. The positive relative differences (i.e., GIM > T-J) at night represent the plasmaspheric contribution to GPS TEC, which is maximized, reaching up to 100% of the corresponding T-J TEC values in the early morning sector. In particular, the relative differences decreased with increasing solar activity, and this may indicate that the plasmaspheric contribution to the maintenance of the nighttime ionosphere does not increase with solar activity, which is different from what we normally anticipate.

**Citation:** Jee, G., H.-B. Lee, Y. H. Kim, J.-K. Chung, and J. Cho (2010), Assessment of GPS global ionosphere maps (GIM) by comparison between CODE GIM and TOPEX/Jason TEC data: Ionospheric perspective, *J. Geophys. Res.*, *115*, A10319, doi:10.1029/2010JA015432.

## 1. Introduction

[2] With the unprecedented spatial and temporal coverage of the observations based on the 24 satellites and corresponding ground stations distributed over the globe, the GPS-based ionospheric total electron content (TEC) data have been extensively utilized in ionospheric studies to analyze and validate the ionospheric models and for space weather monitoring applications. Using TEC data from hundreds of GPS/GLONASS stations worldwide, global ionosphere maps (GIMs) were developed to produce instantaneous snapshots of the global ionospheric TEC. They have been used for monitoring global ionosphere as a key component of the space weather. There are four different versions of GIMs constructed by the Ionosphere Associate Analysis Centers (IAACs): CODE (Center for Orbit Determination in Europe, Astronomical Institute, University of Bern, Switzerland), ESOC/ESA (European Space Operations Center from European Space Agency, Darmstadt, Germany), JPL (Jet Propulsion Laboratory, Pasadena, California, USA), and UPC (Technical University of Catalonia, Barcelona, Spain). For the construction of GIMs, they all have used TEC data obtained from the distribution of the worldwide GPS stations, which are intrinsically biased toward the continents in the Northern Hemisphere but very sparse in the Southern Hemisphere and over the entire ocean (see Figure 1). These data gaps are mostly filled by using appropriate interpolation techniques, and the different versions of GIM are computed independently with different approaches [e.g., *Mannucci et al.*, 1998; *Schaer*, 1999; *Hernández-Pajares et al.*, 1999; *Hernández-Pajares et al.*, 2009]. Furthermore, uncertainties in the GPS TEC are unavoidable from the conversion procedure of slant TEC to vertical TEC [*Mannucci et al.*, 1998; *Mushini et al.*, 2009; E. Kim et al.,

[1]Division of Polar Climate Sciences, Korea Polar Research Institute, Incheon, South Korea.
[2]Also at Department of Space and Astronomy, Chungnam National University, Daejeon, South Korea.
[3]Department of Space and Astronomy, Chungnam National University, Daejeon, South Korea.
[4]Space Geodesy Research Group, Korea Astronomy and Space Science Institute, Daejeon, South Korea.


0148-0227/10/2010JA015432

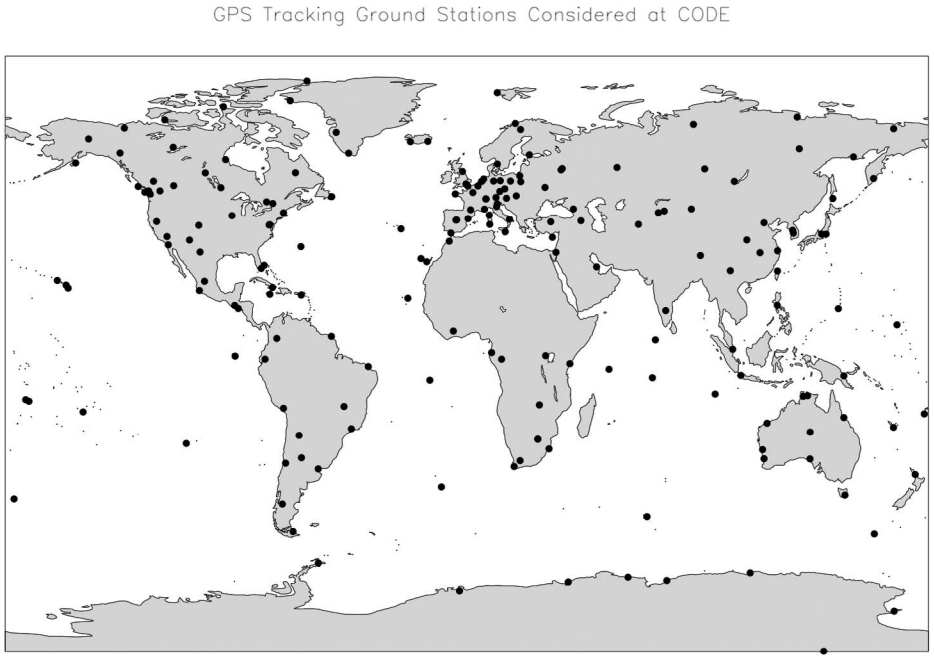


**Figure 1.** GPS ground stations considered at Center for Orbit Determination in Europe (CODE) (obtained from the CODE Web site). For this comparison study, the total electron content (TEC) values from the CODE global ionosphere maps (GIMs) based on these stations were selected at the location and time of T-J satellite orbits (see Figure 2).

A climatology study on ionospheric F2 peak over Anyang, Korea, submitted to *Earth, Planets, and Space*, 2010].

[3] There have been a number of studies to evaluate the performance of the GIMs using independent measurements of the ionospheric TEC such as TOPEX TEC data and climatological models such as Bent and IRI models [e.g., *Ho et al.*, 1997; *Hernández-Pajares et al.*, 1999; *Orús et al.*, 2002, 2003; *Sekido et al.*, 2003]. *Ho et al.* [1997] investigated the accuracy of JPL GIMs by comparing them with the TOPEX TEC measurements and Bent model for the periods of two TOPEX 10 day cycles (10–20 March and 6–16 August 1993). They found that the GIMs agree with the TOPEX measurements much better than the Bent model and the differences between the GIMs and TOPEX TEC are very small, less than 1.5 TECU ($10^{16}$ electrons/$m^2$), depending on distance from the GPS stations. *Orús et al.* [2002] also studied the performance of different kinds of models available for a GNSS single-frequency user, including the International Reference Ionosphere (IRI), the GPS broadcast model, and GPS data-driven GIM models. By comparing with TOPEX data for about 2 years from June 1998 to August 2001, they found that the GIMs show the best performance among these models. However, most of the previous studies on the validation of GIMs have been performed on the basis of only short periods of observation and mainly over the continents where the GPS ground stations are relatively dense. There are few validation studies performed using a long-term database for a climatological comparison over the global ionosphere. In order to assess the overall accuracy of the GIMs in estimating the global ionospheric TEC, we carried out a comprehensive comparison of a GIM model with the TEC data from TOPEX and Jason-1 satellites for the periods of 1998–2008. The TOPEX/Jason (T-J) observations are independent and direct measurements of vertical TEC from ground to satellite altitude over the global ocean and known to be one of the most accurate TEC data currently available. Figure 2 shows the ground tracks of the TOPEX (or Jason) satellite orbit for 10 days, which covers only the global ocean within ±66° in geographic latitude. Therefore, the ocean-based T-J TEC data provide an excellent opportunity to assess the performance of GIMs especially over the global ocean where the GPS ground stations are very sparse. For the comparison with the T-J TEC data, we used GPS TEC taken from CODE GIM at the locations and times of TOPEX/Jason satellite orbits and performed climatological comparisons for different local times, seasons, and solar activities. The results of our study will be presented in terms of general morphology of the global ionosphere for each geophysical condition. In addition, the longitudinal variability of the ionospheric electron density such as the Weddell Sea Anomaly and longitudinal wave structure will also be compared in the global TEC maps from both data. In the following sections, we describe the T-J TEC and CODE GIM as well as the data preparation for this comparison study before presenting our results.

## 2. Data

### 2.1. TOPEX/Jason TEC

[4] The TOPEX/Jason TEC data is a by-product of the satellite radar altimetry missions to measure the surface height of the global oceans from a dual-frequency radar altimeter that is self-consistently correcting the ionospheric delay effect by computing the total electron content along the raypath from the satellite to the sea surface [*Fu et al.*,

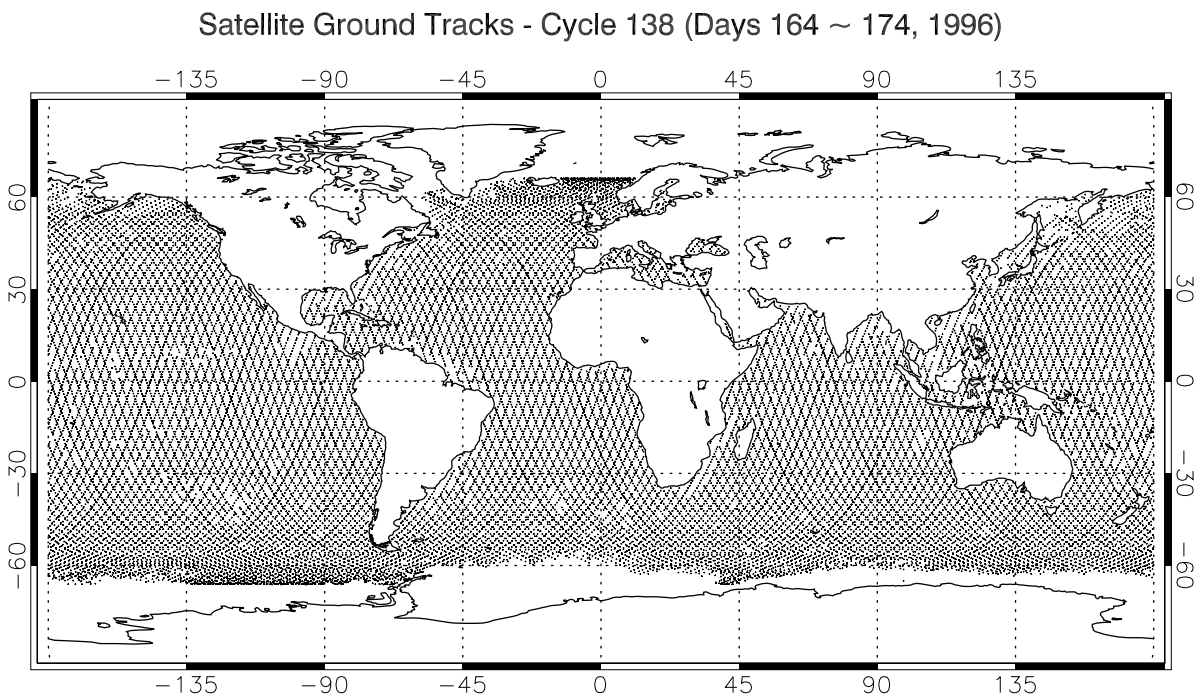


**Figure 2.** TOPEX satellite ground tracks for a 10 day cycle from day 164 to 174 in 1996 (obtained from http://www.jason.oceanobs.com). The Jason satellite has an orbit identical to the TOPEX for better intercalibration and data continuity.

1994]. The TOPEX satellite had been working for more than a full solar cycle from August 1992 to October 2005 when it stopped providing data and was eventually turned off in January 2006. From the great success of this satellite mission, a follow-on mission, Jason-1, was launched on December 2001 and has continued to provide the same quality of TEC data as the TOPEX mission. Jason-1 has an identical orbit to that of the TOPEX satellite for better intercalibration and data continuity; that is, it is taking the orbit of the TOPEX satellite, which shifted its orbit to midway between its original ground tracks on September 2002. Jason-1 is still working on providing high-quality data and its follow-on satellites, Jason-2 and Jason-3, have been already launched (in June 2008) and confirmed for commitment on the mission (for 2013–2014), respectively, to ensure continuity with TOPEX and Jason-1. These series of altimetry satellites will ensure the continuity of the ionospheric TEC measurements for unprecedented periods of time, more than two decades, with consistent data quality. The T-J TEC over the global ocean have provided an excellent complementary ionospheric measurement to conventional measurements, such as ground-based GPS TEC and ionosonde electron density observations, which are mostly collected over the global continents. In this section, only a brief introduction to the TOPEX/Jason TEC measurements will be provided; details of the TOPEX mission and its TEC measurement can be found in previous studies [see *Fu et al.*, 1994; *Codrescu et al.*, 1999; *Jee et al.*, 2004].

[5] The TOPEX satellite carried a dual-frequency radar altimeter operating at 13.6 GHz (Ku band) and 5.3 GHz (C band) simultaneously. In order to remove the ionospheric delay effect, the altimeter estimates the electron content along the raypath from the satellite to the sea surface by measuring the travel times of the radio waves at the two frequencies. The derived electron content is equivalent to the total electron content of the ionosphere in a column extending from the satellite to the sub-satellite reflection point on the surface of the ocean. The TOPEX satellite was orbiting the earth at an altitude of 1336 km with an inclination angle of 66° and a period of 112 min. There are 127 orbits in each 9.916 day period (i.e., 10 day cycle: the satellite passes vertically over the same location, to within 1 km, every ten days), which was chosen as a compromise between spatial and temporal resolutions. The orbit was close to Sun-synchronous, advancing by 2°/d, and it therefore took about 90 days to cover all local times, considering both ascending and descending nodes. The Jason-1 satellite is almost identical to the TOPEX satellites except that it includes a GPS receiver which enables it to measure TEC from Jason to GPS satellites. The TEC data from the TOPEX and Jason-1 satellites were obtained from the NASA Physical Oceanography Distributed Active Archive center at the Jet Propulsion Laboratory (JPL PO.DAAC/NASA). The TEC data were originally taken almost every second along the satellite orbit, which were then averaged for 18 seconds or about 1° of orbit along the satellite path. The resulting 18 s averaged data have a fairly constant spread of about ±4 ~ 5 TECU for different seasons, local times, and hemispheres [*Jee et al.*, 2004]. For each 18 s data point, the corresponding geomagnetic coordinates were computed by adopting quasi-dipole coordinates [*Richmond*, 1995]. It should be noted that the T-J TEC measurements are known to have a systematic bias of 2 ~ 5 TECU above the real ionospheric TEC values from comparisons with other independent TEC measurements [*Codrescu et al.*, 2001; *Orús*

*et al.*, 2002]. In our study, this bias was taken into account by subtracting 4 TECU from the 18 s averaged TEC.

### 2.2. CODE GIM

[6] Global ionospheric maps (GIMs) used in this study were generated on a daily basis at CODE using TEC data from about 200 GPS/GLONASS sites of the International GNSS Service (IGS) and other institutions. Figure 1 displays the global coverage of the GPS tracking ground stations considered at CODE. The vertical TEC is modeled in a solar-geomagnetic reference frame using a spherical harmonic expansion up to degree of order 15. Piecewise linear functions are used for representation in the time domain. The time interval of their vertices is 2 hours, which produces 2 hourly snapshots of the global ionosphere. Each TEC map has a spatial resolution of 2.5° × 5° in the geographic latitude and longitude. Instrumental biases, so-called differential P1-P2 code biases (DCB), for all GPS satellites and ground stations are estimated as constant values for each day, simultaneously with the 13 × 256 or 3328 parameters used to represent the global VTEC distribution. The DCB datum is defined by a zero-mean condition imposed on the satellite bias estimates. P1-C1 bias corrections are taken into account if needed. To convert line-of-sight TEC into vertical TEC, a modified single-layer model (MSLM) mapping function approximating the JPL extended slab model mapping function is adopted. Since March 2002, CODE applied a 3 day combination analysis, solving for 37 × 256 or 9472 VTEC parameters rather than 24 hour analysis for the representation of the global VTEC distribution. Therefore, CODE GIMs correspond to the results for the middle day of three consecutive days. This improvement minimized discontinuities at day boundaries for the achievement of a time-invariant quality level. In addition to this improvement, the CODE GIM has been improved with the increase in the number of GPS ground stations for the TEC data, from only a little more than 100 at the beginning to about 240 stations. However, we have not considered these improvements of GIMs but included all the GIM TEC for this comparison study at various geophysical conditions. Details on the CODE GIM can be found on the web (http://aiuws.unibe.ch/ionosphere) as well as in the work of *Schaer* [1999]. We utilized CODE GIMs for periods from March 1998 to May 2009 in this study.

## 3. Analysis

[7] While CODE GIMs continually produce 2 hourly snapshots of the global ionosphere, the TOPEX/Jason satellites measure TEC along the satellite orbit that is advancing only by 2° per day (that is, almost Sun-synchronous). Given the entirely different characteristics of two data sets, a direct comparison between them cannot be made. Therefore, one of the data sets has to be adjusted for the comparison. Since it is not possible to produce a 2 hourly snapshot of the global ionosphere with the TOPEX/Jason observations along their satellite orbits, GPS TEC from the CODE GIMs were selected at each 18 s TOPEX/Jason data points along the satellite orbit for the periods of March 1998 to May 2009. A simple linear interpolation was applied for the GPS TEC values between two successive 2 hourly GIMs. Now, all the 18 s T-J TEC have corresponding GPS TEC obtained from GIMs, and they can be directly compared with each other. For the comparison, the data were binned for three solar activities ($F10.7 \leq 100$, $100 < F10.7 \leq 150$, $F10.7 > 150$) and four seasons (March equinox for the days of 35 to 125 around March 21, June solstice for the days of 126 to 218 around June 21, September equinox for the days of 219 to 309 around September 22, and December solstice for the days of 310 to 34 around December 21). We performed the comparison only for geomagnetically quiet periods ($K_p < 3$) since this type of climatological analysis cannot reveal the effects of geomagnetic activity on the ionosphere [*Jee et al.*, 2004].

## 4. Results and Discussion

[8] Figures 3a–3c show the global TEC maps from GIM and T-J TEC measurements and their differences for low ($F10.7 < 100$), medium ($100 < F10.7 < 150$), and high ($F10.7 > 150$) solar activity levels, respectively. Each case has four seasonal conditions: March equinox, June solstice, September equinox and December solstice, from top to bottom of Figures 3a–3c. The TEC maps are displayed in the geomagnetic latitude and local time coordinate (with 2° × 0.25 hour bins), which were calculated by using quasi-dipole coordinates [*Richmond*, 1995]. There are two kinds of difference maps in Figure 3: the absolute differences between two sets of TEC (GIM-T-J in TECU) and the percentage or relative differences with respect to the TOPEX/Jason data ((GIM-T-J)/T-J in percentage). On average, GIM seems to be able to reproduce the spatial and temporal variations of the global ionosphere as well as the seasonal variations such as the annual and semiannual anomalies for all solar activities. However, the difference maps show systematic discrepancies between the two sets of TEC. The most noticeable difference in Figure 3 is the existence of negative values in the difference maps. Since the orbit altitude of GPS satellites (20,200 km) is higher than that of TOPEX/Jason satellites (1336 km), GIM TEC is supposed to be larger than the T-J TEC; however, the difference maps show not only positive values (i.e., GIM > T-J) but also negative values (i.e., GIM < T-J). The latter reaches up to more than 50% of the T-J TEC at middle and high latitudes and occurs during the most of local times except for the middle of the day. Although the negative differences are only 3–5 TECU in the absolute difference maps, it should be noted that this is the result from the "average" TEC maps rather than from the instantaneous snapshots of the ionosphere. The negative differences are much more significant for low solar activity than for high solar activity conditions. They are also stronger in the Southern Hemisphere than in the Northern Hemisphere, especially in the southern winter, probably owing to the very sparse GPS ground stations in the Southern Hemisphere (see Figure 1). This might be considered as a fundamental limitation of the GPS-based GIMs, which cannot be improved unless the additional GPS ground stations are provided in the data-sparse regions.

[9] The anticipated results from this comparison study are the positive differences (i.e., GIM > T-J) due to the different top boundaries of the measurements, that is, 1336 km and 20,200 km altitudes for the TOPEX/Jason and GPS satellites, respectively. The altitude region between two satellite orbits approximately belongs to the plasmasphere.

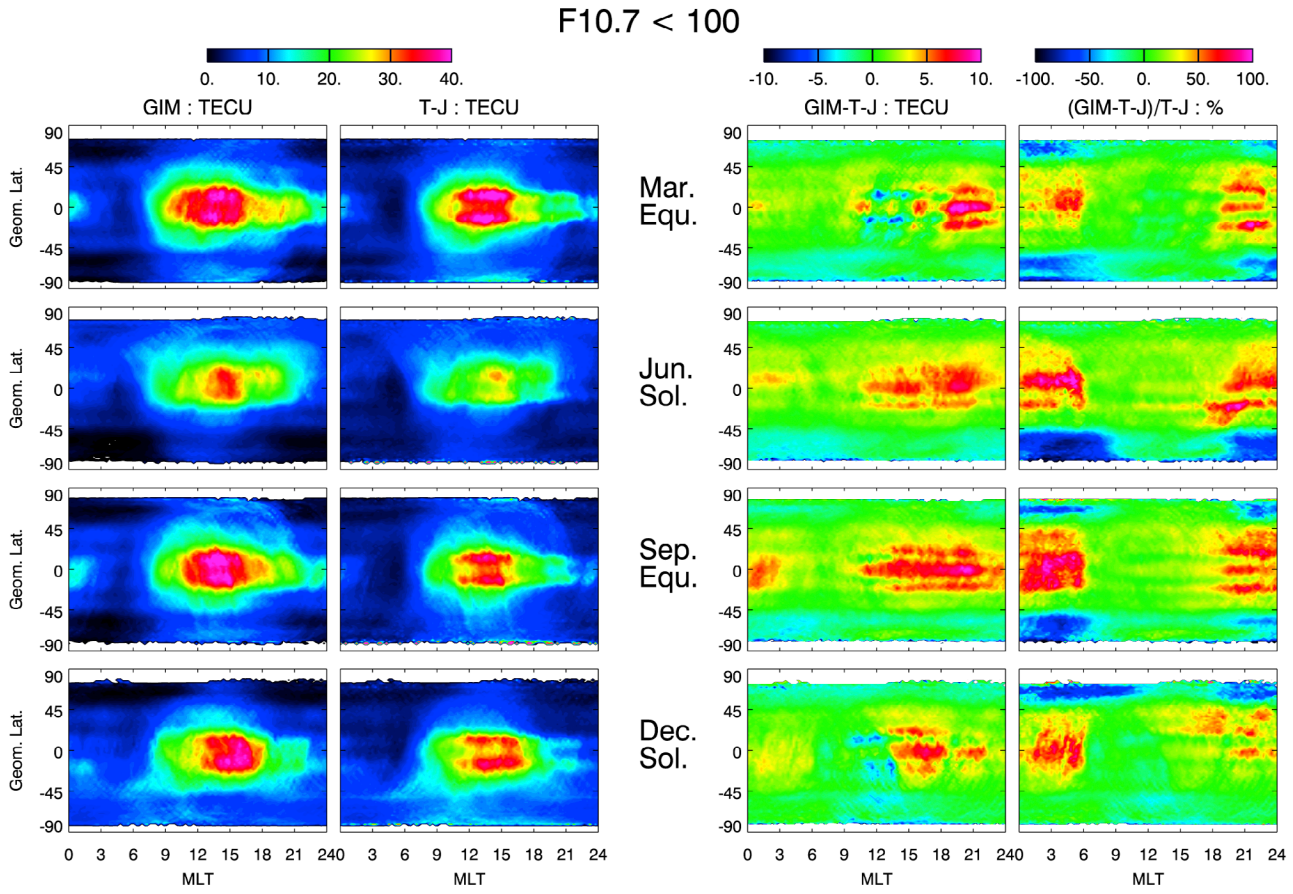


**Figure 3a.** Global TEC maps for low solar activity ($F10.7 \leq 100$) produced from the GPS GIM model and TOPEX/Jason data. Four seasonal cases are displayed from top to bottom: March equinox, June solstice, September equinox, and December solstice. Each TEC map is constructed in the geomagnetic latitude and local time coordinate.

Therefore, the electron contents in the region (i.e., positive differences) may be regarded as the plasmaspheric electron density, which can influence the ionospheric total electron density, especially at night. In the absolute difference maps, the positive differences seem to be closely correlated with the equatorial anomaly structures reproduced from the two TEC data sets. The equatorial anomaly structures in the GIM TEC maps are not well represented for low solar activity in Figure 3a, almost nonexistent from the afternoon all the way to the midnight, while the T-J TEC maps present relatively clear anomaly crests and trough. Even for the higher solar activity conditions in Figures 3b and 3c, the overall anomaly structures in the GIM TEC maps are much weaker than those in the T-J TEC maps, and the anomaly crests after sunset are not as distinguished as in the T-J TEC maps. This discrepancy results in large positive differences over the anomaly trough and the poleward of the anomaly crests and as negative differences over the anomaly crests for all high solar activity levels. *Ho et al.* [1997] performed a statistical comparison between GIM and TOPEX TEC by using TOPEX TEC data for two 10 day cycles and the corresponding GPS data. Their results showed that the accuracy of GIMs was low in the equatorial and southern hemispheric regions, which were explained by the inadequacies of the shell model in the presence of large latitudinal gradients as in the equatorial region and the small number of GPS stations in the ocean area. Their estimation of the mean TEC difference in the equatorial region was around 3.8 TECU, which was interpreted as the contribution of the plasmasphere. We also found that the accuracy of GIM TEC is relatively low over the equatorial and southern hemispheric regions, but the maximum differences in our results, appearing at the trough of the equatorial anomaly, are much larger than theirs: it is as large as 10 TECU for low solar activity and goes beyond 15 TECU for high solar activity.

[10] The relative or percentage difference maps in Figures 3a–3c (right) show the relative magnitude of the TEC differences with respect to the T-J TEC. In these maps, the most distinguished differences occur at night and both positive and negative differences can be as large as up to 100% of the T-J TEC. Note that the large daytime absolute differences at low latitudes are not significant compared with the daytime ionospheric TEC (i.e., T-J TEC), which appear small in the relative difference maps in Figures 3a–3c. However, the seemingly small nighttime absolute differences are the most noticeable differences in the relative difference maps. These large relative differences at night are not surprising since it is well known that the downward flux of the plasmaspheric

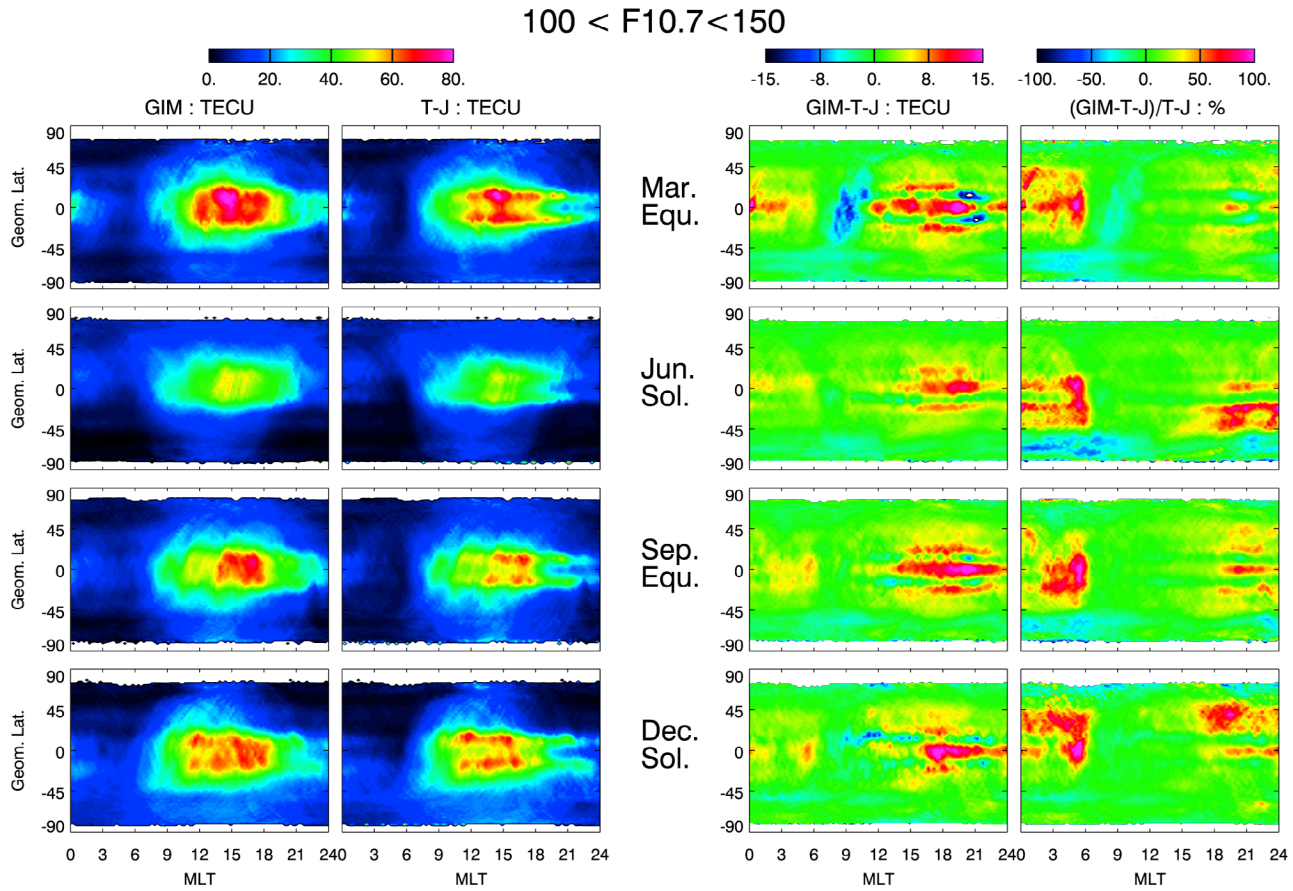


**Figure 3b.** Same as Figure 3a, but for medium solar activity ($100 < F10.7 \leq 150$). Note that the color scales are different from Figure 3a.

electron density to the ionosphere significantly contributes to the maintenance of the nighttime ionosphere and can be as important as the effect of neutral winds [*Jee et al.*, 2005]. Assuming that the downward flux is largely proportional to the relative magnitude of the plasmaspheric electron density compared with the ionospheric density, the relative positive differences in Figure 3 may be regarded as an indicator of the plasmaspheric contribution to the maintenance of the nighttime ionosphere. According to this assumption, the largest contribution seems to occur in the early morning sector (0–6 magnetic local time (MLT) in the TEC maps) where the plasmaspheric densities are almost comparable to the ionospheric densities especially for low solar activity.

[11] As the solar activity increases, the ionospheric electron densities increase because of the enhanced photoionization and so does the upward flux of the ionospheric electrons to the plasmasphere during the day. Therefore, it is logical to anticipate that the nighttime downward plasmaspheric flux will also be enhanced with increasing solar activity. However, our results show that although the absolute positive differences at night increase with solar activity, the corresponding relative differences do not increase with increasing solar activity. Instead, they decrease from almost 100% of the T-J TEC during low solar activity to less than 50% during high solar activity in the early morning sectors. Since the positive relative differences from GPS to T-J are closely related with the downward plasmaspheric flux, this result may indicate that the plasmaspheric contribution to the maintenance of the nighttime ionosphere does not increase with solar activity. By comparing two independent simultaneous measurements of ground-based GPS TEC and Jason-1 GPS TEC measuring TEC from Jason to GPS satellites, *Yizengaw et al.* [2008] found that the relative contribution of the plasmaspheric TEC to GPS TEC increases with solar activity, reaching up to 60% at solar maximum but reducing to less than 35% at solar minimum, which is contrary to our result. However, it should be noted that their result was based on only three months of different solar activity conditions (October 2003, May 2005, and December 2006) while our result was based on the TEC data for nearly 10 years from March 1998 to May 2009, which covers almost a full solar cycle. Further study is required to identify how the plasmaspheric downward flux varies with solar activity.

[12] The TEC maps in Figures 3a–3c are presented in the geomagnetic latitude and local time coordinate, which were comprised of the longitudinally averaged TEC values and

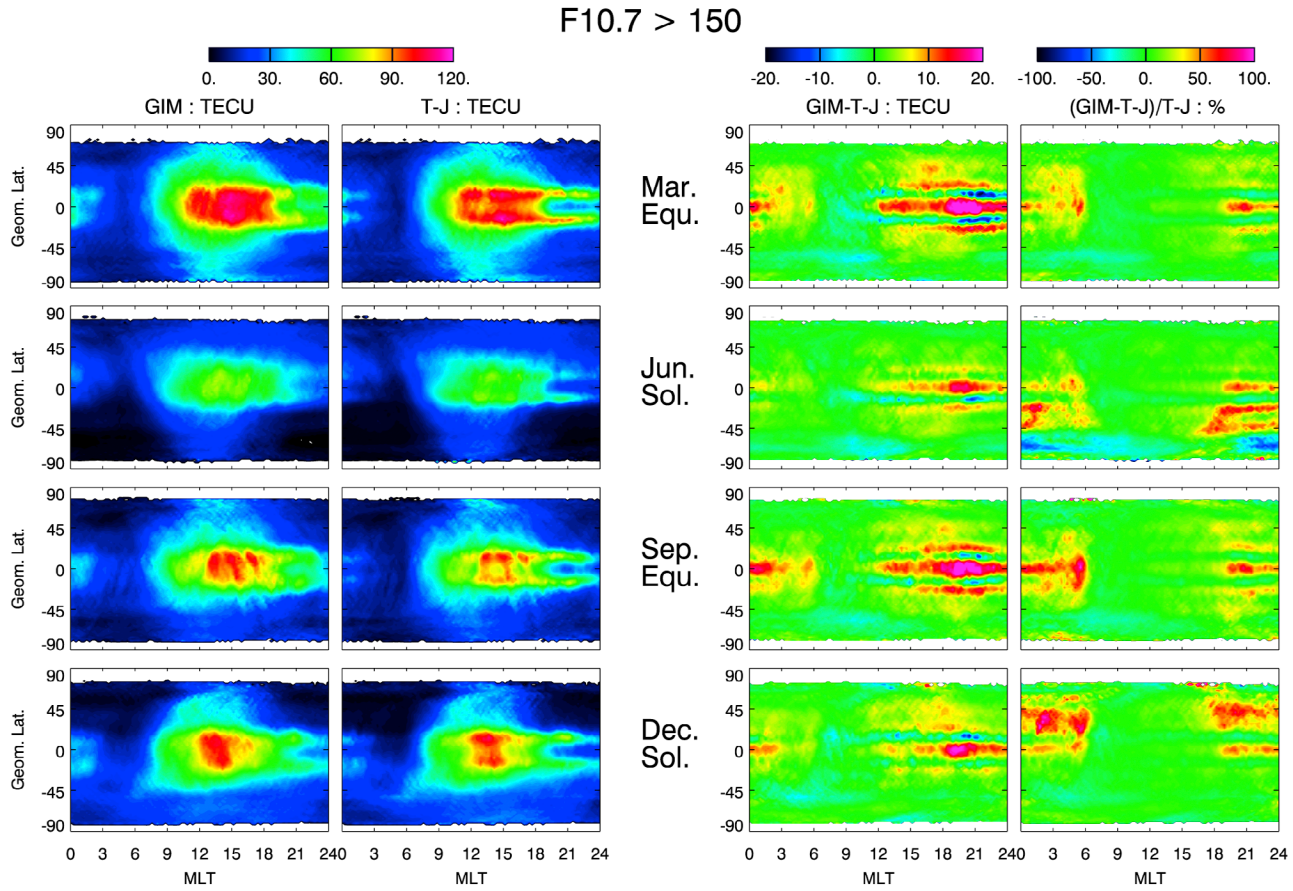


**Figure 3c.** Same as Figure 3a, but for high solar activity ($F10.7 > 150$). Note that the color scales are different from Figures 3a and 3b.

thus were not able to show any longitudinal variability of the global ionosphere. In the subsequent figures, the TEC maps are displayed in the latitude and longitude coordinates for the comparison study on the longitudinal variability such as the Weddell Sea Anomaly (WSA) and longitudinal wave structures. The TEC maps for WSA are displayed in the geomagnetic latitude and longitude coordinate (with 2° × 3.75° bins) for low and high solar activities in Figures 4a and 4b, respectively. Since the WSA is characterized by higher nighttime electron densities in the longitude region near the Weddell Sea, this figure shows TEC maps at noon (left panels) and midnight (right panels) local time sectors as the representatives of day and night. This structure is well reproduced in the southern summer (December solstice) with density enhancements around 130° ~ 180° longitude below South America. This nighttime density enhancements from the T-J TEC data are evidently greater than the corresponding daytime values by up to about 30% for low and 70% for high solar activities. The GIM TEC maps also show the WSA for low solar activity: the nighttime TEC is slightly larger than or comparable to the daytime values in the WSA region. However, for high solar activity, it merely shows much broader and weaker density enhancements than the WSA in the corresponding T-J TEC map. Furthermore, the density enhancement in the GIM map ranges largely over the entire southern Pacific and Atlantic sectors, while the WSA in the T-J map is confined to the Pacific sector, especially within the eastern Pacific.

[13] Note that the WSA is usually presented in the geographic coordinate since it was, as implied by the name, considered as a local phenomenon, which appeared only at a specific geographic location near the Weddell Sea. The local nature of the WSA is also related to the fact that it was initially observed by the local ground-based ionosonde data near the Antarctic Peninsula and Wedell Sea before the satellite measurements revealed the global view of the ionosphere [*Horvath and Essex*, 2003, and references therein]. However, recent studies indicate that the formation of the WSA is strongly correlated with the geomagnetic field structure [*Horvath*, 2006; *Jee et al.*, 2009]. Therefore, it may be more appropriate to display the WSA in the geomagnetic coordinate for better interpretation as in Figure 4. Originally, the WSA was known to appear only in the southern summer [*Horvath and Essex*, 2003]. As the solar activity increases, however, the T-J TEC maps seem to show the nighttime density enhancements in the WSA region even for the equinox periods, though less distinguished than that in summer (see Figure 4b). In the Northern Hemisphere, it is

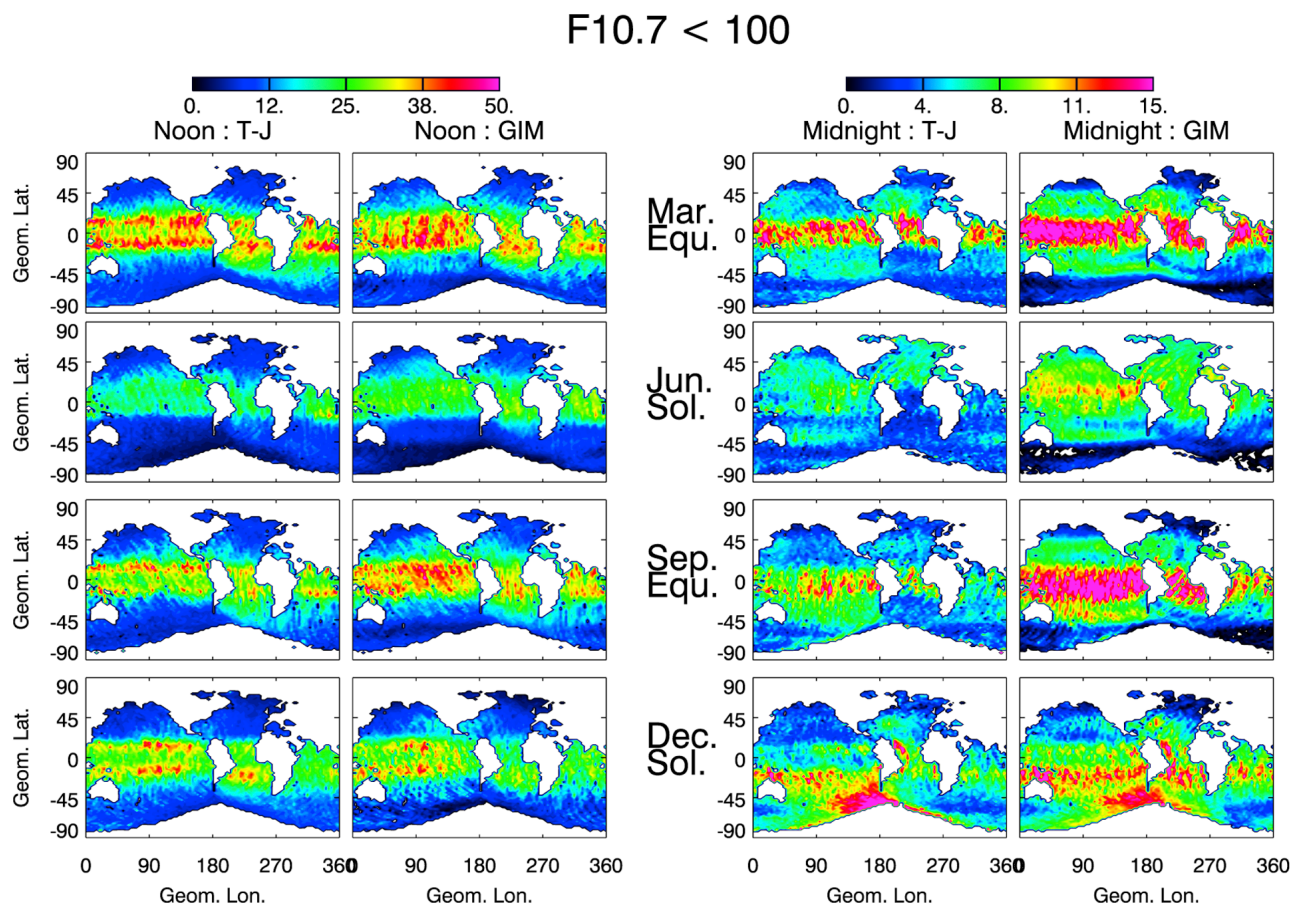


**Figure 4a.** Global TEC maps for (left) noon and (right) midnight local time sectors, displayed in the magnetic latitude and longitude coordinates for low solar activity ($F10.7 \leq 100$). These maps are constructed from the T-J and GIM TEC data to show the Weddell Sea Anomaly for March equinox, June solstice, September equinox, and December solstice (from top to bottom).

hard to see any WSA-like structure even in summer in both TEC data sets. *Lin et al.* [2009] reported from the analysis of the Constellation Observing System for Meteorology, Ionosphere and Climate (COSMIC) observations for 2007 that they found the WSA-like structure in the northern summer hemisphere, specifically at the East Asian sector as well as in the southern WSA region. In their study, however, the level of TEC enhancements in the Northern Hemisphere cannot be compared with the enhancements of the WSA; it was much weaker and disappeared quickly, even before the midnight local time sectors. With regard to the WSA-like structures, the fundamental difference between the Southern Hemisphere and the Northern Hemisphere is the geometrical characteristics of the geomagnetic field lines as described by *Jee et al.* [2009]. Although the TEC maps in Figures 4a and 4b show very limited northern midlatitude ionosphere, nighttime density enhancements over the Atlantic sector in the northern summer are common (around 45° magnetic latitude (MLAT) and 180°~240° magnetic longitude (MLON) for June solstice), but they are neither as significant as the WSA nor larger than the daytime values of these figures. In the study of the nighttime plasma enhancements of the northern midlatitude ionosphere by using the multi-instrument data from the Defense Meteorological Satellite Program (DMSP), *Horvath and Lovell* [2009] also concluded that the WSA-like structures in the Northern Hemisphere are only common midlatitude nighttime enhancements occurring over the northern summer hemisphere but not the northern equivalent of the WSA.

[14] There is another longitudinal variability of the global ionosphere, rather recently discovered, called the longitudinal wave number 4 structure or, simply, the longitudinal wave structure [*Sagawa et al.*, 2005; *Scherliess et al.*, 2008; *Kim et al.*, 2008, and references therein]. Figure 5 shows the longitudinal wave structure at low and midlatitudes (less than ±45° geographic latitude) for the local time sector of 1200–1800 hours when the equatorial anomaly is best developed. The longitudinal wave structures are closely correlated with the formation of the equatorial anomaly that is well developed in the T-J TEC maps but not very noticeable, especially for low solar activity, in the GIM TEC maps (see Figure 3). As shown by *Scherliess et al.* [2008] and *Kim et al.* [2008], who utilized the TOPEX TEC data for their study, the T-J TEC maps show clear longitudinal wave structures for both solar activities: wave number 4 (e.g., June solstice and September equinox) and wave number 3 (e.g., March equinox and December solstice). However, the GIM TEC maps do not display these wave

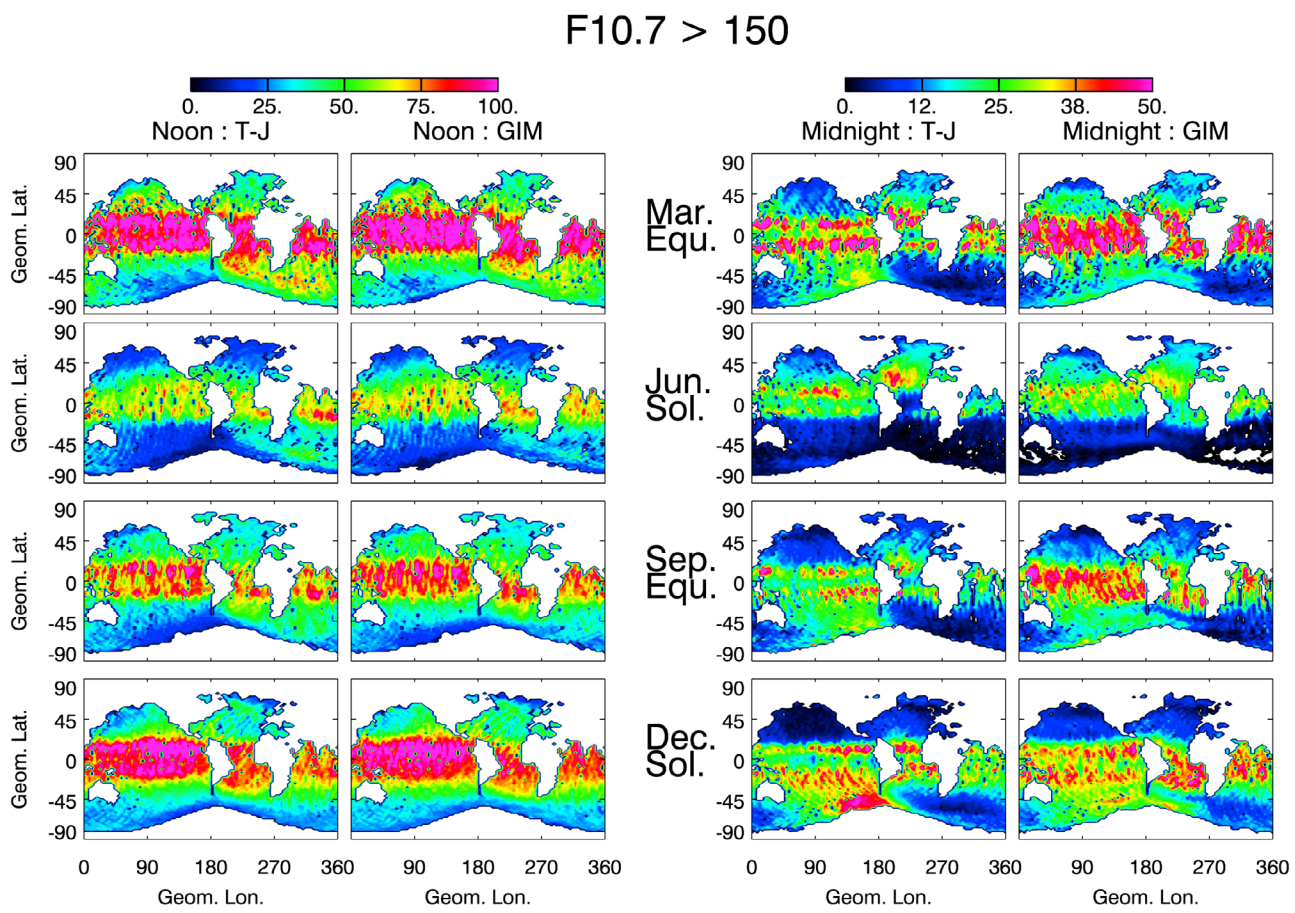


**Figure 4b.** Same as Figure 4a, but for high solar activity ($F10.7 > 150$). Note that the color scales are different from Figure 4a.

structures nor show any significant longitudinal variations along the equatorial anomaly region. The results in Figures 4 and 5 show that the GIM TEC are not accurate enough to reproduce the longitudinal variabilities of the global ionosphere such as the WSA and the longitudinal wave structure, which are well reproduced in the T-J TEC data.

## 5. Summary and Conclusion

[15] By comparing with the TOPEX/Jason TEC measurements, we have evaluated the performance of the GPS-based CODE GIM model especially over the global ocean where the GPS ground stations are sparse and mathematical schemes are used with the GIM model to estimate TEC. We utilized 10 year T-J TEC data from March 1998 to May 2009 for various geophysical conditions including local time, latitude/longitude, season, and solar activity. On the whole, the GIM model was largely able to reproduce the spatial and temporal variations of the global ionosphere as well as the seasonal variations such as the annual and semiannual anomalies for all solar activities. However, the GIM model was not accurate enough to represent well-known ionospheric structures such as the equatorial anomaly, the Weddell Sea Anomaly (WSA), and the longitudinal wave structure.

[16] The equatorial anomaly was not well represented in the GIM TEC maps, being almost nonexistent from the afternoon all the way to the midnight during low solar activity, while the T-J TEC maps presented relatively clear anomaly crests and trough (Figure 3a). Even during the higher solar activities, the overall anomaly structures in the GIM TEC maps were much weaker than those in the T-J TEC maps, and the anomaly crests after sunset were not as distinguished as in the T-J TEC maps (Figures 3b and 3c). The T-J TEC maps were able to very clearly reproduce the WSA in southern summer for all solar activities and during equinox periods for high solar activity, but the GIM TEC maps could reproduce the WSA only in summer for low solar activity (Figures 4a and 4b). The T-J TEC maps clearly show the longitudinal wave number 4 (e.g., June solstice and September equinox) and wave number 3 (e.g., March equinox and December solstice) structures, but the GIM TEC maps do not show any significant longitudinal variations along the equatorial anomaly region (Figure 5).

[17] Furthermore, there seems to be a fundamental limitation of the GIM model in the northern high-latitude and the southern middle- and high-latitude regions, which are mostly

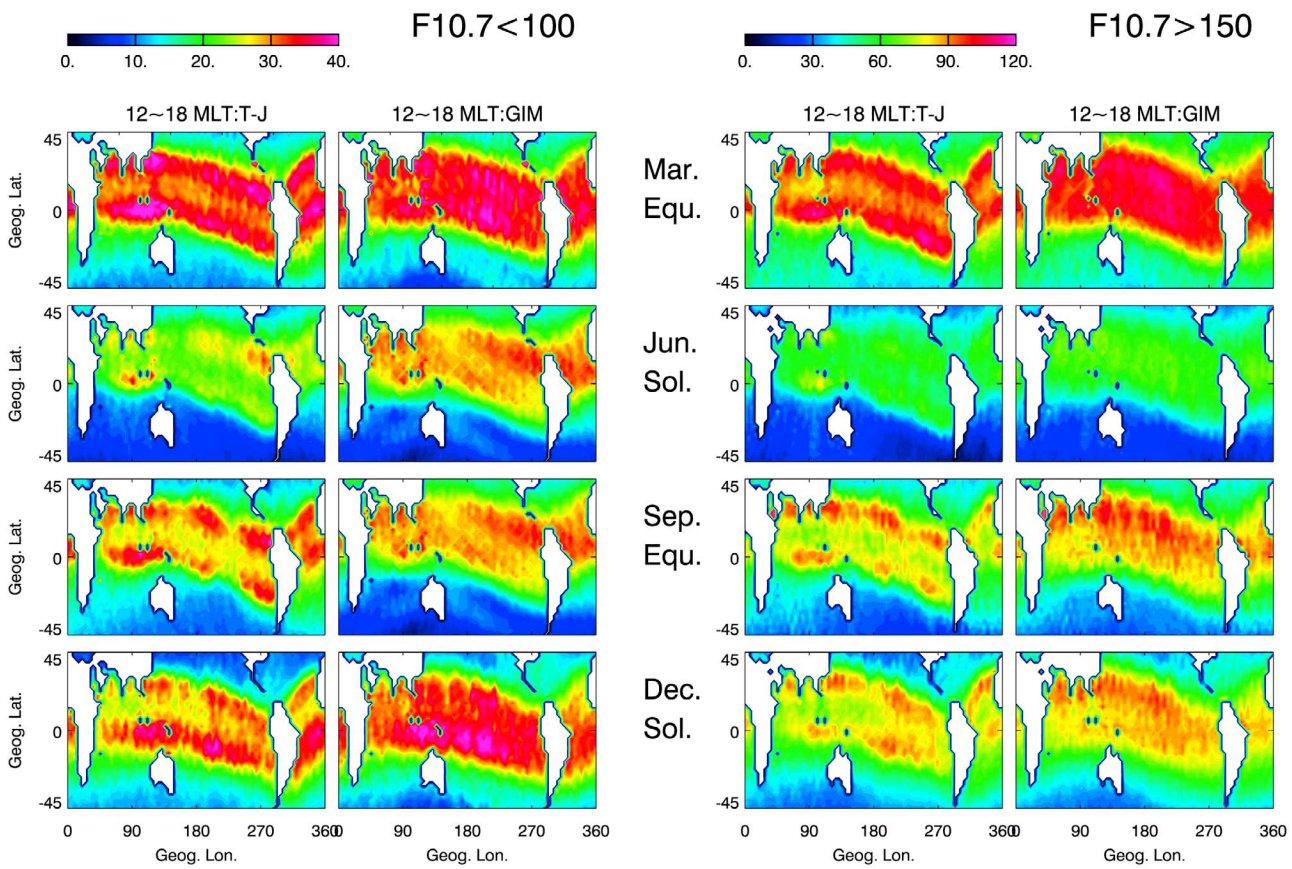


**Figure 5.** TEC maps for presenting the longitudinal wave structures displayed at low and midlatitudes (less than ±45° geographic latitude) and for the local time sector of 1200~1800 LT when the equatorial anomaly is best developed. These maps are shown for the (left) low and (right) high solar activity conditions.

occupied by oceans and include very sparse GPS ground stations. In these regions, the GPS TEC is even smaller than the T-J TEC, by more than 50%, despite the higher top measurement boundary of the GPS TEC (20,200 km) compared to the T-J TEC (1336 km). The negative differences (i.e., GPS < T-J) are stronger for low solar activity than for high solar activity conditions.

[18] With regard to the positive TEC differences (i.e., GPS > T-J) in the equatorial and low-latitude regions, they represent the plasmaspheric electron content between 1336 km and 20,200 km altitudes. In particular, the nighttime positive values of the relative differences (i.e., percentage differences from GIM to T-J TEC in Figure 3) may represent the plasmaspheric contribution to the maintenance of the nighttime ionosphere. These nighttime positive differences are maximized, reaching up to 100% in the early morning sector. Our result also shows that as solar activity increased, the relative positive differences did not increase with solar activity but rather decreased from almost 100% of the T-J TEC for low solar activity to less than 50% for high solar activity although the absolute positive differences at night increased with solar activity. This result may indicate that the plasmaspheric contribution to the maintenance of the nighttime ionosphere does not increase with increasing solar activity, which is different from what we normally anticipate.

[19] As a final remark on the quality of GPS GIMs, it has continually improved because of the increasing number of ground stations used for GPS TEC data and updated mapping techniques. However, we utilized all CODE GIM TEC maps currently available for better statistics. Therefore, the most recent GPS GIMs may show better performance in representing the global ionosphere than the results of this study.

[20] **Acknowledgments.** This work was supported by Korea Research Council of Fundamental Science and Technology Grant (PG09050 at KOPRI and 1345086367 at KASI). Y.H.K acknowledges support from KOPRI through the Composition of Polar Atmospheric and Climate Change (COMPAC). The TOPEX/Jason TEC data were obtained from the NASA Physical Oceanography Distributed Active Archive Centre (PO.DAAC) at the NASA Jet Propulsion Laboratory, Pasadena, California (http://podaac.jpl.nasa.gov), and the CODE GIMs were obtained from the Crustal Dynamics Data Information System (CDDIS) at Goddard Space Flight Center, NASA.

[21] Robert Lysak thanks Ildiko Horvath and another reviewer for their assistance in evaluating this manuscript.

## References

Codrescu, M. V., S. E. Palo, X. Zhang, T. J. Fuller-Rowell, and C. Poppe (1999), TEC climatology derived from TOPEX/POSEIDON measurements, *J. Atmos. Sol. Terr. Phys.*, *61*, 281–298.

Fu, L. L., E. J. Christensen, and C. A. Yamarone Jr. (1994), TOPEX/Poseidon mission overview, *J. Geophys. Res.*, *99*(C12), 24,369–24,381.

Hernández-Pajares, M., J. M. Juan, and J. Sanz (1999), New approaches in global ionospheric determination using ground GPS data, *J. Atmos. Sol. Terr. Phys.*, *61*, 1237–1247.

Hernández-Pajares, M., J. M. Juan, J. Sanz, R. Orús, A. Garcia-Rigo, J. Feltens, A. Komjathy, S. C. Schaer, and A. Krankowski (2009), The IGS VTEC maps: A reliable source of ionospheric information since 1998, *J. Geod.*, *83*, 263–275. doi:10.1007/s00190-008-0266-1.

Ho, C. M., B. D. Wilson, A. J. Mannucci, U. J. Lindqwister, and D. N. Yuan (1997), A comparative study of ionospheric total electron content measurements using global ionospheric maps of GPS, TOPEX radar, and the Bent model, *Radio Sci.*, *32*, 1499–1512.

Horvath, I. (2006), A total electron content space weather study of the nighttime Weddell Sea Anomaly of 1996/1997 southern summer with TOPEX/Poseidon radar altimetry, *J. Geophys. Res.*, *111*, A12317, doi:10.1029/2006JA011679.

Horvath, I., and E. A. Essex (2003), The Weddell Sea Anomaly observed with the Topex satellite data, *J. Atmos. Sol. Terr. Phys.*, *65*, 693–706.

Horvath, I., and B. C. Lovell (2009), An investigation of the Northern Hemisphere midlatitude nighttime plasma density enhancements and their relations to the midlatitude nighttime trough during summer, *J. Geophys. Res.*, *114*, A08308, doi:10.1029/2009JA014094.

Jee, G., R. W. Schunk, and L. Scherliess (2004), Analysis of TEC data from the TOPEX/Poseidon mission, *J. Geophys. Res.*, *109*, A01301, doi:10.1029/2003JA010058.

Jee, G., R. W. Schunk, and L. Scherliess (2005), On the sensitivity of total electron content (TEC) to upper atmospheric/ionospheric parameters, *J. Atmos. Sol. Terr. Phys.*, *67*, 1040–1052.

Jee, G., A. G. Burns, Y.-H. Kim, and W. Wang (2009), Seasonal and solar activity variations of the Weddell Sea Anomaly observed in the TOPEX total electron content measurements, *J. Geophys. Res.*, *114*, A04307, doi:10.1029/2008JA013801.

Kim, E., G. Jee, and Y. H. Kim (2008), Seasonal characteristics of the longitudinal wave number 4 structure in the equatorial ionospheric anomaly, *J. Astron. Space Sci.*, *25*, 335–346.

Lin, C. H., J. Y. Liu, C. Z. Cheng, C. H. Chen, C. H. Liu, W. Wang, A. G. Burns, and J. Lei (2009), Three-dimensional ionospheric electron density structure of the Weddell Sea Anomaly, *J. Geophys. Res.*, *114*, A02312, doi:10.1029/2008JA013455.

Mannucci, A. J., B. D. Wilson, D. N. Yuan, C. H. Ho, U. J. Lindqwister, and T. F. Runge (1998), A global mapping technique for GPS-derived ionospheric total electron content measurements, *Radio Sci.*, *33*, 565–582.

Mushini, S. C., P. T. Jayachandran, R. B. Langley, and J. W. MacDougall (2009), Use of varying shell heights derived from ionosonde data in calculating vertical total electron content (TEC) using GPS: New method, *Adv. Space Res.*, *44*, 1309–1313.

Orús, R., M. Hernández-Pajares, J. M. Juan, J. Sanz, and M. García-Fernández (2002), Performance of different TEC models to provide GPS ionospheric corrections, *J. Atmos. Sol. Terr. Phys.*, *64*, 2055–2062.

Orús, R., M. Hernández-Pajares, J. M. Juan, J. Sanz, and M. García-Fernández (2003), Validation of the GPS TEC maps with TOPEX data, *Adv. Space Res.*, *31*, 621–627.

Richmond, A. D. (1995), Ionospheric electrodynamics using magnetic apex coordinates, *J. Geomagn. Geoelectr.*, *47*, 191–212.

Schaer, S. (1999), Mapping and predicting the Earth's ionosphere using the global positioning system, Ph.D. dissertation, Astron. Inst. Univ. of Bern, Switzerland.

Scherliess, L., D. C. Thompson, and R. W. Schunk (2008), Longitudinal variability of low-latitude total electron content: Tidal influences, *J. Geophys. Res.*, *113*, A01311, doi:10.1029/2007JA012480.

Sekido, M., T. Kondo, E. Kawai, and M. Imae (2003), Evaluation of GPS-based ionospheric TEC map by comparing with VLBI data, *Radio Sci.*, *38*(4), 1069, doi:10.1029/2000RS002620.

Yizengaw, E., M. B. Moldwin, D. Galvan, B. A. Iijima, A. Komjathy, and A. J. Mannucci (2008), Global plasmaspheric TEC and its relative contribution to GPS TEC, *J. Atmos. Sol. Terr. Phys.*, *70*, 1541–1548.

J. Cho and J.-K. Chung, Space Geodesy Research Group, Korea Astronomy and Space Science Institute, Daejeon, 305-348, South Korea.

G. Jee and H.-B. Lee, Center of Climate Sciences, Korea Polar Research Institute, Incheon, 406-840, South Korea. (ghjee@kopri.re.kr)

Y. H. Kim, Department of Space and Astronomy, Chungnam National University, Daejeon, 305-764, South Korea.